

Robust Model Predictive Control for Aircraft Intent-Aware Collision Avoidance

Arash Bahari Kordabad, Andrea Da Col, Arabinda Ghosh, Sybert Stroeve, and Sadegh Soudjani

Abstract—This paper presents the use of robust model predictive control for the design of an intent-aware collision avoidance system for multi-agent aircraft engaged in horizontal maneuvering scenarios. We assume that information from other agents is accessible in the form of waypoints or destinations. Consequently, we consider that other agents follow their optimal Dubin’s path—a trajectory that connects their current state to their intended state—while accounting for potential uncertainties. We propose using scenario tree model predictive control as a robust approach that offers computational efficiency. We demonstrate that the proposed method can easily integrate intent information and offer a robust scheme that handles different uncertainties. The method is illustrated through simulation results.

I. INTRODUCTION

Aircraft, from commercial airliners to private jets, are indispensable across industries like transportation, tourism, and logistics, facilitating efficient passenger and cargo transport and supporting global commerce with their manned or unmanned flight capabilities. However, the safe integration of various types of aircraft in shared airspace remains a paramount concern. With the increasing volume of air traffic, path planning and control for multi-agent aircraft systems are vital for safe, efficient, and coordinated navigation in shared airspace, handling high traffic volumes, and reducing accident risks. These air-traffic systems determine optimal routes and maneuvers to avoid collisions, using centralized strategies or decentralized strategies [1]. Some key challenges including managing dynamic environments, ensuring real-time response, and handling uncertainties in aircraft behavior, are often addressed by mathematical optimization [2]. These issues are crucial for advanced air traffic management and the safe integration of diverse aircraft types [3]. Research efforts have been dedicated to the development of advanced technologies and protocols to mitigate collision risks and improve the safety of airspace operations [4]–[6].

In order to ensure safe and efficient operations for multi-agent aircraft, having a reliable collision avoidance system (CAS) is crucial. Some studies concentrated on providing CAS against static obstacles [7], whereas others incorporated moving obstacles [8]. CAS are designed based on centralized or decentralized strategies. Centralized strategies mostly consists of non-cooperative UAVs, manage collision

avoidance with a single control entity, and ensures the optimal airspace use in the expense of significant computational resources. On the contrary, decentralized systems offer a cooperative approach which leads to scalability and robustness. Here, UAVs are allowed to independently determine its path while communicating with others. Thus, compared to noncooperative approaches, cooperative methods enhance situational awareness and decision-making [9]. Existing literature featured both cooperative and non-cooperative approaches like Palmer et al. proposed both centralized and decoupled approaches for cooperative collision avoidance of UAVs [10], Wang et al. proposed a reinforcement learning approach for path-planning while avoiding obstacles in noncooperative decentralized scenarios [11]. Lindqvist et al. proposed a nonlinear model predictive control (MPC) for path planning and dynamic obstacle avoidance for unmanned aerial vehicles (UAVs) [12]. However, this work did not address the uncertainties in the trajectories of the dynamic obstacles.

In the context of multi-agent control, integration of intent awareness is a cooperative strategy. It involves obtaining and understanding the information of the intentions of humans and/or autonomous agents. This understanding is then integrated into planning and control algorithms [13]. Such insight into intent helps in planning and decision-making, allowing for better anticipation and adaptation to the actions of other agents. Many previous methods lack the capability to comprehend the intentions of humans or other agents with whom they interact, potentially resulting in inefficiencies, misinterpretations, or even unsafe behavior in dynamic and uncertain environments [14]. In the current literature, intent awareness is primarily used in human-robot interaction, where the main goal for an autonomous agent is to comprehend human intentions and execute designated tasks [15], [16]. However, in the context of multi-agent planning and control, especially in air traffic management of UAVs, the use of intent awareness is not explored, which serves as the primary motivation for this paper.

On the industrial side, airborne collision avoidance systems (ACAS) are critical safety measures designed to prevent mid-air collisions between aircraft. These systems use transponder signals to detect the presence of other aircraft, calculate potential collision threats, and provide pilots with real-time avoidance instructions. The ACAS X program represents the next generation of these systems, introducing enhanced algorithms and more advanced technology to improve accuracy and reduce unnecessary alerts. ACAS X includes various versions tailored for different aviation sectors, such as ACAS Xa for large aircraft and ACAS Xu for unmanned aerial

Arash Bahari Kordabad, Andrea Da Col, Arabinda Ghosh, and Sadegh Soudjani are with the Max Planck Institute for Software Systems, Kaiserslautern, Germany. E-mail: {arashbk, adacol, arabinda, sadegh}@mpi-sws.org. Sybert Stroeve is with the Royal Netherlands Aerospace Centre NLR. E-mail: Sybert.Stroeve@nlr.nl. This research is supported by the following grants: EIC 101070802 and ERC 101089047.

systems [17], [18]. The threat resolution module in ACAS X employs optimized decision logic tables that are generated offline using Dynamic Programming (DP) [19]. DP optimizes decision-making under uncertainty, breaking down complex problems into manageable subproblems to find the optimal solution efficiently. It plays a crucial role in environments where the outcomes are uncertain and when interacting with other agents whose behaviors are dynamic [20]. However, it might be computationally complex for large-scale systems [21]. On the contrary, Model Predictive Control (MPC) offers the advantage of real-time optimization by solving control problems at each time step, allowing for dynamic adjustment based on current state information. Unlike DP, MPC can handle constraints and adapt to changes in the system model and environment efficiently. This makes MPC more suitable for complex, real-time applications. Scenario-tree MPC is a robust MPC technique designed to handle finite and discrete uncertainties in a nonlinear system [22]. It extends traditional MPC by explicitly considering multiple possible future scenarios, typically represented in a tree structure. Scenario-tree MPC offers a computationally tractable strategy for handling uncertainty in future discrete scenarios, allowing for approximate robust decision-making [23]. Scenario-tree MPC can then potentially provide an approximate solution for the DP [24].

In this paper, we consider the horizontal maneuvering of multi-agent aircraft system. Our primary objective is to incorporate intent information into the planning and control of collision avoidance systems for unmanned aerial vehicles in shared airspace. We first formulate intent awareness as information on waypoints available to other agents. A robust MPC strategy is then applied to the system to obtain an optimal path for aircraft collision avoidance, considering the intent information. Specifically, we propose the use of scenario-tree MPC as an approximate yet robust solution for the aircraft collision avoidance problem. Then, the intent information can be used to predict the trajectory of the MPC scheme, providing a computationally tractable approach.

The paper is structured as follows. Section II presents a background on the classic MPC and scenario-tree MPC approaches. Section III describes the equations of motion and dynamics for horizontal maneuvering UAVs. Section IV elaborates on intent awareness and demonstrates how it can be integrated into the CAS. Moreover, an intent-aware robust MPC is presented in this section. Section V provides the simulation results, and section VI delivers a conclusion.

II. BACKGROUND

In this section, we provide a background on the classic and scenario tree MPC approaches.

A. Model Predictive Control (MPC)

Model Predictive Control (MPC) is a powerful optimization-based control method that produces control policies by solving an optimal control problem at each discrete time instant based on the current system state s , over a finite, receding horizon. As one of the main benefits, MPC can

directly account for state-input constraints in optimization with computational efficiency, especially for deterministic systems. For deterministic dynamics, the problem is often formulated as:

$$\min_{\hat{s}, \hat{a}} V_f(\hat{s}_N) + \sum_{k=0}^{N-1} L(\hat{s}_k, \hat{a}_k) \quad (1a)$$

$$\text{s.t. } \forall k \in \{0, \dots, N-1\} :$$

$$\hat{s}_{k+1} = \mathbf{f}_d(\hat{s}_k, \hat{a}_k), \quad \hat{s}_0 = \mathbf{s} \quad (1b)$$

$$\mathbf{h}(\hat{s}_k, \hat{a}_k) \leq 0, \quad \hat{a}_k \in \mathcal{A}, \quad (1c)$$

where L is the stage cost, V_f is the terminal cost, \mathbf{f}_d is the deterministic dynamics model, \mathbf{h} is the constraints, N is the horizon length and \mathcal{A} is the control set. In order to distinguish between the actual system trajectory and the predicted state-input profile, we use the notation $\hat{\cdot}$ for the latter. The open-loop optimization (1) is solved recursively at each state s and produces a complete profile of control inputs $\hat{\mathbf{a}}^* = \{\hat{\mathbf{a}}_0^*, \dots, \hat{\mathbf{a}}_{N-1}^*\}$ and corresponding state predictions $\hat{\mathbf{s}}^* = \{\hat{\mathbf{s}}_0^*, \dots, \hat{\mathbf{s}}_N^*\}$. The notation *star* \cdot^* is used to refer to the optimal value of the decision variables. To incorporate feedback, only the first element $\hat{\mathbf{a}}_0^*$ of the input sequence $\hat{\mathbf{a}}^*$ is applied to the system, a successor state s^+ is attained in the next time instance, and the optimization (1) is solved again for the new state s^+ . Therefore, MPC-based policy refers to the following policy:

$$\pi_{\text{MPC}}(s) = \hat{\mathbf{a}}_0^*.$$

It is evident that a deterministic model, such as \mathbf{f}_d used in MPC (1), is unable to capture the stochastic nature and uncertainties. Therefore, it is limited in situations where there are no significant uncertainties and relatively small disturbances in the system, as it typically relies on deterministic models. Consequently, it is necessary to employ a notion of robust MPC for nonlinear systems that is computationally efficient. Note that, based on the online receding horizon nature of the MPC, there are circumstances where traditional MPC can still perform acceptably, even in stochastic systems. This is often the case when the system uncertainties are relatively small, predictable, or can be well approximated by the deterministic model used by the MPC. In the following, we will introduce an efficient and robust MPC approach.

B. Scenario-tree MPC

In this section, we detail scenario-tree MPC as a computationally tractable robust MPC for nonlinear systems.

Consider m samples from a distribution W , denoted by w^i , and suppose that a stochastic system is approximated by the following set of dynamics:

$$s^+ = \mathbf{f}(s, \mathbf{a}, w^i), \quad i \in \{1, \dots, m\}. \quad (2)$$

Therefore, there will be different trajectories based on the possible w^i at each time instance. The number of trajectories (scenarios) grows exponentially with the length of the MPC horizon. Accordingly, it is common to fix the uncertain parameters after a certain period of time called the robust horizon $N_r < N$. Note that in this section, the superscript

denotes the scenario index. Figure 1 illustrates the evolution of the system represented as a scenario-tree for $m = 3$, $N_r = 2$, and $N = 3$. Each scenario corresponds to a specific trajectory, starting from the root (current state) to a leaf. Each node in the tree represents a possible state of the system at a future time step, and each branch represents a possible transition due to the uncertain parameter w^i with $i \in \{1, 2, 3\}$. The uncertain parameter is fixed to w^1 after $N_r = 2$ steps.

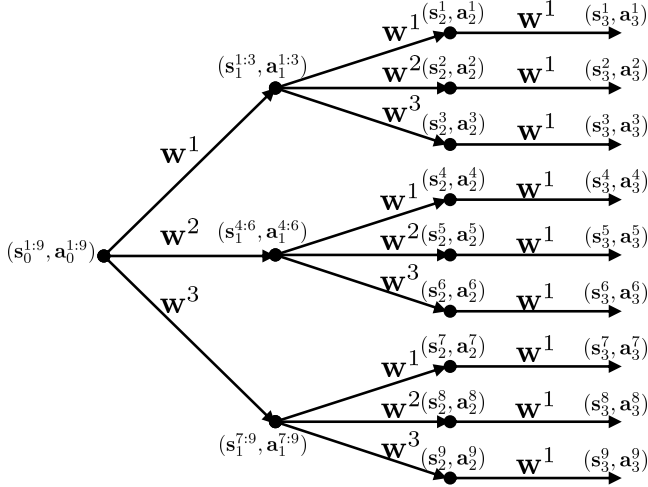


Fig. 1. The evolution of the system represented as a scenario-tree.

The number of all scenarios is $M = m^{N_r}$, and in the figure, there are 9 different scenarios. The superscripts in the states denote a specific scenario, while the subscripts are used for the time index. The notation $s_k^{i:j}$ denotes $s_k^i = s_k^{i+1} = \dots = s_k^j$. For instance, in the beginning, all scenarios start with the current specific state that is denoted by $s_0^{1:9}$. Furthermore, since uncertainty cannot be predicted in advance, control actions must depend solely on historical realizations of uncertainty. Hence, $a_i^j = a_i^l, \forall i = 0, \dots, k$, if the uncertainty realization for scenarios j and l are identical up to and including time stage k . This restriction is commonly referred to as a *non-anticipativity* constraint [22]. This constraint in Figure 1 can be expressed as $a_0^{1:9}, a_1^{1:3}, a_1^{4:6}$, and $a_1^{7:9}$.

Considering all scenarios in the constraints and optimizing the cost function based on their average, the scenario-tree MPC optimization can be expressed as follows:

$$\begin{aligned} \min_{\hat{s}, \hat{a}} \quad & \sum_{j=1}^M \left(V_f(\hat{s}_N^j) + \sum_{k=0}^{N-1} L(\hat{s}_k^j, \hat{a}_k^j) \right), \\ \text{s.t.} \quad & \forall k \in \{0, \dots, N-1\}, \forall j \in \{1, \dots, M\}: \\ & \hat{s}_{k+1}^j = f(\hat{s}_k^j, \hat{a}_k^j, w^i), \quad \hat{s}_0^j = s \\ & h(\hat{s}_k^j, \hat{a}_k^j) \leq 0, \quad \hat{a}_k^j \in \mathcal{A}, \\ & \forall l \in \{1, \dots, M\}, \forall i \in \{0, \dots, k\}: \\ & \hat{a}_k^j = \hat{a}_k^l \quad \text{if} \quad \hat{s}_i^j = \hat{s}_i^l, \end{aligned}$$

where

$$i = \begin{cases} \text{mod}(\lceil \frac{j}{m^{N_r-k-1}} \rceil, m) & k < N_r \\ N_r \leq k, \end{cases}$$

indicates the index of parameter w^i for each time-scenario pair, and where the function $1 \leq \text{mod}(n, m) \leq n$ is the remainder of n/m if n/m is not an integer, otherwise $\text{mod}(n, m) = m$. Moreover, $\lceil n \rceil := \min\{m \in \mathbb{Z} \mid m \geq n\}$.

Analogous to the standard MPC, the policy of robust MPC based on a scenario-tree is determined as follows:

$$\pi_{\text{RMPC}}(s) = \hat{a}_0^{1:M,*},$$

where $\hat{a}_0^{1:M,*}$ is the optimal solution of $\hat{a}_0^1 = \dots = \hat{a}_0^M$.

III. EQUATIONS OF MOTION

In this section, we provide the equations of motion for two aircraft in the horizontal plane maneuvering. We consider two aircraft, ownship and intruder, to have the following equation of motion in the discrete-time setting:

$$s_{k+1}^i := \begin{bmatrix} x_{k+1}^i \\ y_{k+1}^i \\ \sigma_{k+1}^i \end{bmatrix} = \begin{bmatrix} x_k^i \\ y_k^i \\ \sigma_k^i \end{bmatrix} + t_e \begin{bmatrix} v_k^i \cos \sigma_k^i \\ v_k^i \sin \sigma_k^i \\ u_k^i \end{bmatrix}, \quad i \in \{1, 2\}, \quad (3)$$

where the superscript $i = 1$ stands for the ownship whereas $i = 2$ corresponds to the intruder, s_k^i is the state of the aircraft i at time k , x_k^i and y_k^i are the position states, and σ_k^i is the heading angle. The constant t_e is the sampling time and is assumed to be 1 sec, and v_k^i and u_k^i are the linear and angular velocities, respectively. Figure 2 shows the geometry of the problem.

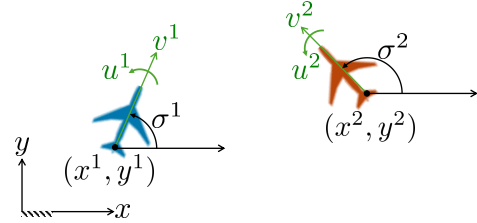


Fig. 2. Geometry of two aircraft in the horizontal plane in the earth-fixed coordinate system. The black variables are the state variables and the greens are the velocities.

Action space (\mathcal{A}): We consider the linear and angular velocities as control inputs. Although discrete advisories (i.e., control inputs) are used more frequently in the DP approach [25], the MPC approach requires solving an optimization problem at each time instance. In the MPC scheme, it is preferable to have decision variables in the continuous space to avoid the computational complexity associated with discrete variables and mixed-integer programming. Therefore, a continuous set $\mathcal{A} = [6, 9][\text{m/s}] \times [-0.1, 0.1][\text{rad/s}]$ is considered for the ownship, and $\mathcal{A} = 10[\text{m/s}] \times [-0.07, 0.07][\text{rad/s}]$ is used for the intruder.

Uncertainties: Uncertainties in aircraft dynamics typically manifest additively in the angular velocity. Specifically, the actual advisory is typically considered to be the nominal value with a relatively high probability (e.g., 0.5), and the

endpoints of the intervals have a relatively lower probability (e.g., 0.25). This type of uncertainty is used in DP approaches due to its discrete nature, making it easier to address numerically [25]. In this paper, we consider a similar way of uncertainty modeling for the intruder with equal probability for the scenario-tree MPC approach as a robust MPC. More specifically, we assume that the intruder may adopt either a nominal angular velocity or the angular velocities at the boundaries to form the branches of the scenario-tree MPC.

IV. INTENT-AWARE SCENARIO-TREE MPC

In this paper, one of our main contributions is the consideration of scenarios where the ownship is aware of the intruder's intent in the MPC scheme. This intent is modeled as the intruder's future path, or equivalently, its upcoming control inputs, which are available to the ownship. Specifically, the intent is represented as a series of waypoints that the intruder will pass through. Using these waypoints, the overall path is determined based on the Dubins path, which is the optimal path that connects the intruder's current position to the next waypoint [26].

The Dubins path is tangent to the initial conditions (position and direction) and the next waypoint. It determines the path by specifying maneuvers such as turning left (L) by a certain angle, moving straight (S) for a specific duration, and finally turning right (R) by a certain angle. Figure 3 illustrates an example of such a path, denoted as LSR. The gray dashed-line circles represent the maximum possible curvature based on the limitations of linear and angular speed. Both geometric [27] and analytical methods [28] are available to compute this optimal path. More specifically, the optimal Dubin's path

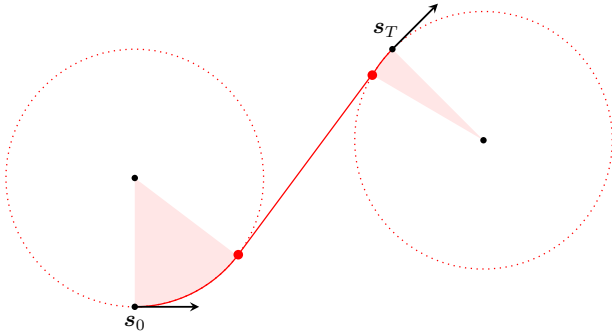


Fig. 3. An LSR Dubins path

provides a mapping from the initial-target state pair to the path connecting these two states, i.e., $(s_0, s_T) \rightarrow (s_0, s_1, \dots, s_T)$ and consequently the angular velocities can be obtained by a certain time-varying mapping, as follows:

$$u_k = D(s_0, s_T, k), \quad 0 \leq k < T,$$

where D is a mapping from the initial state, the target state, and the time index k to the corresponding optimal angular velocity u_k , generating the optimal Dubin's path. This mapping can be obtained based on different types of optimal paths including RSR, RSL, LSR, LSL, RLR, or LRL.

Note that, the linear velocity is assumed to take its maximum value (constant) for optimality purposes.

In the context of MPC, incorporating the intruder's intent information into the control synthesis for the ownship is relatively straightforward. First, the intruder's current state and waypoint are used to determine its Dubin path, which allows for the prediction of the intruder's upcoming control inputs. An MPC scheme is then formulated for the ownship with objectives such as minimizing control effort or reaching a destination, while adhering to constraints such as maintaining a minimum safe distance from the intruder. Consequently, the intruder's dynamics and predicted control inputs are integrated into the ownship MPC scheme. By utilizing the intruder's intent information, these values can be accurately included in the ownship MPC, reducing uncertainty. In contrast, without knowledge of the intruder's intent, predictions are based on assumptions like a direct path for the intruder, which introduces more uncertainty.

For the ownship ($i = 1$), we consider v_k^i and u_k^i as the control input. These velocities are assumed to be obtained based on Dubin's optimal path for the intruder ($i = 2$). Therefore, based on the initial state and the *intent* state for the intruder, we can obtain the corresponding Dubin's path and the corresponding control inputs. Then, the aim is to steer the ownship to its intent state while avoiding collision with the intruder using an MPC method.

In order to incorporate uncertainties that arise from the intruder, when the ownship is at the state s_t , $0 \leq t \leq T$, we utilize an intent-aware scenario-tree MPC approach as follows:

$$\min_{u_{0:N-1}^1, v_{0:N-1}^1, s_{0:N}^1} (s_N^1 - s_T)^\top Q_f (s_N^1 - s_T) + (s_0^1 - s_T)^\top Q (s_0^1 - s_T) \quad (4a)$$

$$+ \sum_{k=1}^{N-1} (s_k^1 - s_T)^\top Q (s_k^1 - s_T) + R(u_k^1 - u_{k-1}^1)^2,$$

$$\text{s.t. } \forall j \in \{1, \dots, M\}, \forall k \in \{0, \dots, N-1\} :$$

$$(3), \quad \forall i \in \{1, \{2, j\}\}, \quad (4b)$$

$$\rho \leq \sqrt{(s_k^1 - s_k^{2,j})^\top \text{diag}(1, 1, 0) (s_k^1 - s_k^{2,j})}, \quad (4c)$$

$$\underline{u}^1 \leq u_k^1 \leq \bar{u}^1, \quad \underline{v}^1 \leq v_k^1 \leq \bar{v}^1, \quad (4d)$$

$$\text{if } k < N_r : u_k^{2,j} = \quad (4e)$$

$$\begin{cases} \bar{u}^2 & \text{if } \text{mod}\left(\left\lceil \frac{j}{3^{N_r - k - 1}} \right\rceil, 3\right) = 0 \\ \underline{u}^2 & \text{if } \text{mod}\left(\left\lceil \frac{j}{3^{N_r - k - 1}} \right\rceil, 3\right) = 1 \\ D(s_0^2, s_T^2, t + k) & \text{if } \text{mod}\left(\left\lceil \frac{j}{3^{N_r - k - 1}} \right\rceil, 3\right) = 2, \end{cases}$$

$$\text{if } k \geq N_r : u_k^{2,j} = D(s_0^2, s_T^2, t + k), \quad (4f)$$

$$v_k^{2,j} = \bar{v}^2, \quad (4g)$$

$$s_0^1 = s_t, \quad (4h)$$

where Q_f and Q are positive definite matrices, R is a positive constant, ρ is the minimum allowed horizontal distance of the two aircraft and \underline{v}^i (\underline{u}^i) is the minimum and \bar{v}^i (\bar{u}^i) is the maximum allowed linear (angular) velocity for $i \in \{1, 2\}$.

Robust MPC (4) steers the ownship state to its target state s_T with a quadratic cost in (4a) while avoiding collision

with the intruder, enforced by the constraint (4c), which is taking its optimal Dubin path with additional uncertainties. The last term in the cost function in (4a) minimizes the variations in the angular velocity. Constraint (4b) represents the dynamics of the ownship ($i = 1$), and dynamics of the intruder for M different scenarios $i \in \{2, j\}$, $j \in \{1, \dots, M\}$ conducted according to Figure 1. Constraint (4d) enforces the control limitations for the ownship. Constraint (4e) generates different inputs (as uncertainties) for three branches ($m = 3$) of the scenario-tree MPC. We have considered an uncertainty for the angular velocity of the intruder in the form of $u_k^2 \in \{\underline{u}^2, D(s_0^2, s_T^2, k), \bar{u}^2\}$ until the robust horizon N_r with $\underline{u}^2 = -0.07$ [rad/s] and $\bar{u}^2 = 0.07$ [rad/s]. After the robust horizon N_r , the intruder follows its optimal dubin's path and (4f) enforces this. The linear velocity for the intruder is assumed to be constant and follows its maximum value, as represented in constraint (4g). Finally, constraint (4h) sets the initial state of the ownship MPC to the actual current state s_t and the MPC is solved in the receding current manner. Note that in MPC (4), because the uncertainties appear in the control input value, there is no need to add the non-anticipativity constraint. This restriction is implicitly accounted for in constraint (4e).

In other words, these M scenarios account for uncertainties in the intruder's execution of angular velocity (i.e., control input) by considering both the nominal angular velocities that follow the optimal Dubins path and the worst-case angular velocities over a few steps ahead (robust horizon). Incorporating these scenarios into the optimization 4 reduces the feasibility domain, leading to more conservative control inputs for the ownship compared to when only the intruder's nominal trajectory is considered. However, this approach enhances robustness against potential uncertainties arising from e.g., human error, mismatches in the intent information, external disturbances, etc.

In cases where intent information is not available or accounted for, a straight-line prediction is typically assumed for the intruder. Thus, in MPC (4), the value of the function D is replaced with zero. This discrepancy between the prediction and the actual path of the intruder can result in a non-optimal path, as it will be demonstrated in the simulation results. It is important to note that considering intent information is beneficial not only for optimization and safety purposes but also for the MPC recursive feasibility. Recursive feasibility in MPC schemes can be challenging when the system is uncertain, such as when the intruder's waypoint does not align with the predicted path. Knowledge of the intruder's intent assists in reducing the uncertainty and, consequently, achieving recursive MPC feasibility.

V. SIMULATION RESULTS

In the next section, we illustrate simulation results for the collision avoidance problem for two aircraft based on the proposed method. Throughout the simulations, we have used a 30s horizon length for the MPC ($N = 30$) and a robust horizon of $N_r = 3$.

Figure 4 compares the ownship nominal trajectory, the path obtained from the classic MPC, and the scenario-tree MPC. In the nominal trajectory, without any intruder present, the ownship follows an LS Dubin optimal path to reach its next waypoint. However, when an intruder exists in the airspace, the path deviates from the optimal nominal path to avoid collisions. The intruder and its corresponding Dubins path are shown in red. It can be seen that both the scenario-tree MPC and the classic MPC successfully avoid collisions with the nominal trajectory of the intruder. However, the scenario-tree approach maintains a greater distance from the nominal path of the intruder compared to the classic MPC approach.

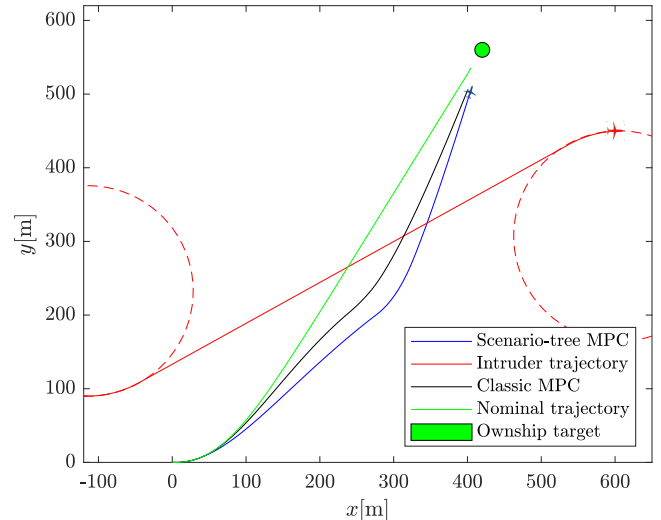


Fig. 4. Comparing the classic MPC trajectory (black), the scenario-tree MPC trajectory (blue), and the nominal trajectory (green) without safety constraints for the ownship. The intruder Dubins path is shown in red and the green area is the destination of the ownship.

Figure 5 shows the distance between the ownship and the intruder. The green curve is for the nominal trajectory, and it can be seen that it violates the safety constraint. Moreover, it can be seen that both the classic and the scenario-tree MPC respect the minimum distance constraint. However, for the scenario-tree MPC, the distance is larger until around 51 seconds. This is the time when the ownship passes behind the intruder, and practically, the scenario-tree MPC no longer affects the trajectory of the ownship after that. A detailed reason is shown in Figure 6, where the top-left (bottom-left) figure is at $t = 35s$, and the top-right (bottom-right) figure is at $t = 57s$ for the scenario-tree (classic) MPC approach. The corresponding predicted trajectories are shown in black.

Figure 7 compares the ownship trajectory in scenarios with (blue) and without (green) the intent information. The intent information about the future trajectory of the intruder can be used to obtain a shorter path for the ownship while avoiding the collision. Note that in this figure, we have used a different encounter scenario than in the other simulation results to provide a clearer illustration of the importance and impact of the intent information.

To demonstrate the robustness of the proposed method,

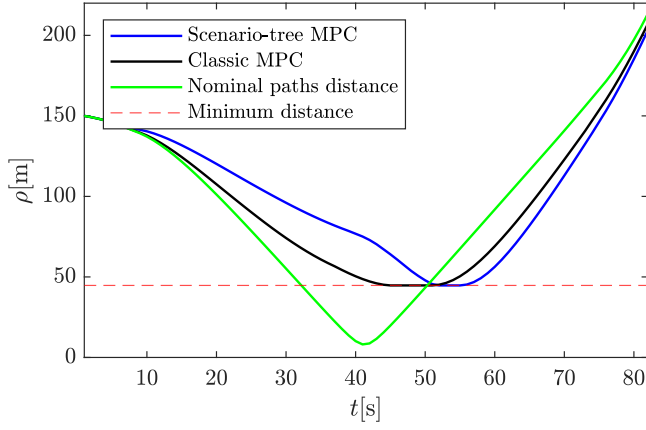


Fig. 5. The distance between the ownship and the intruder over time. The red dashed line is the minimum allowed distance. The green curve is for the nominal path.

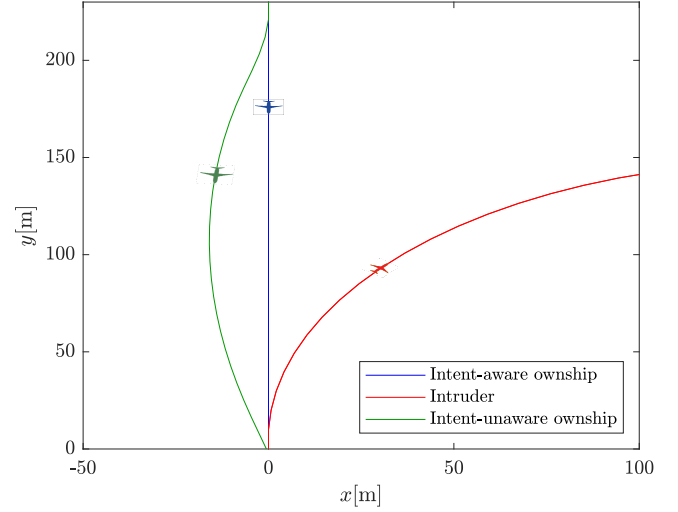


Fig. 7. Comparing the ownship path for the case of with (blue) and without (green) the intent information.

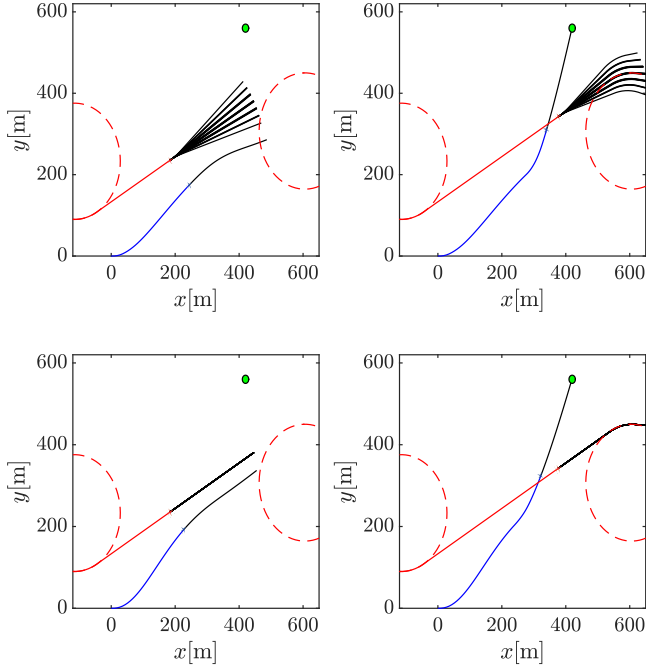


Fig. 6. The top-left (bottom-left) figure shows the trajectories at $t = 35$ s (before passing behind the intruder), and the top-right (bottom-right) figure shows the trajectories at $t = 57$ s, after passing behind the intruder, for the scenario-tree (classic) MPC approach.

we have conducted 20 different simulations for the intruder, incorporating small bounded uniform uncertainties in the angular velocity as follows:

$$u_k^2 = D(s_0^2, s_T^2, k) + 10^{-3}\omega, \quad \omega \sim \mathcal{U}[-1, 1], \quad (5)$$

where \mathcal{U} is the uniform distribution. Such variations can occur, for example, due to errors in the shared waypoints relative to the actual intruder path or deviations from the exact Dubins optimal path by the intruder. The resulting trajectories for the intruder (red) and the corresponding ownship paths (blue)

are depicted in Figure 8. Although the disturbance at each time instance in (5) is relatively small in magnitude, it leads to a fairly significant deviation in the terminal position of the intruder due to the propagation over time, with a difference of around 70 meters as shown in Figure 8. Additionally, it's important to note that, for computational efficiency and to avoid overly conservative control inputs, the robustness of the scenario tree MPC is applied over a fairly short robust horizon rather than the entire maneuvering horizon.

As illustrated in Figure 9, all cases comply with the minimum distance constraint. The nominal trajectories are shown in black.

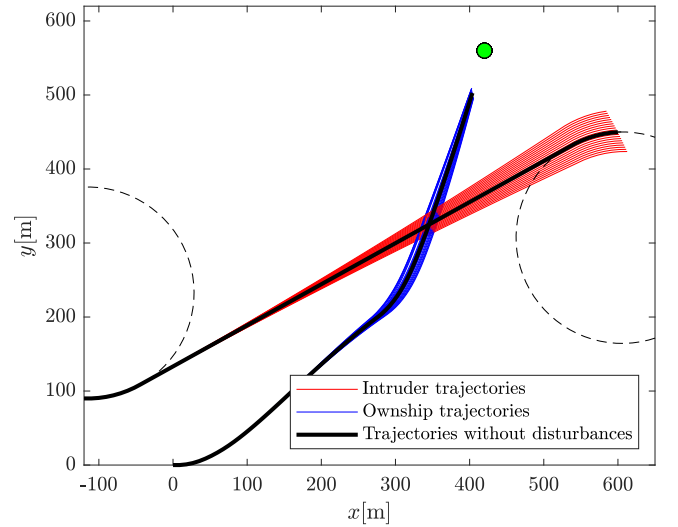


Fig. 8. The intruder (red) and the ownship (blue) trajectories for 20 different cases arise from the intruder's angular velocity uncertainties. The nominal trajectories are shown in black.

Finally, Figure 10 shows the control input for the linear

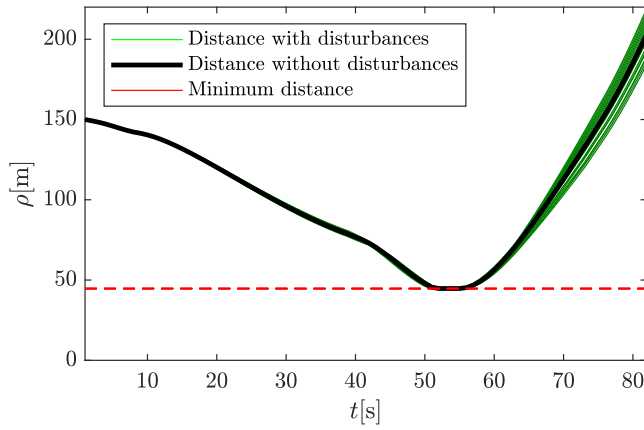


Fig. 9. The distance between the ownship and the intruder over time for different cases. The nominal distance is shown in black.

velocity and angular velocity and their boundaries for the scenario-tree MPC for all the uncertain cases. Note that in the CAS optimal path, the global optimal angular velocity is typically expected to be zero or at the boundary of the permitted interval. Figure 10 generally aligns with this expectation. The slight deviation near zero may be attributed to the nature of the finite-horizon objective in the MPC scheme, which approximates the infinite-horizon objective, as well as to dynamic uncertainties.

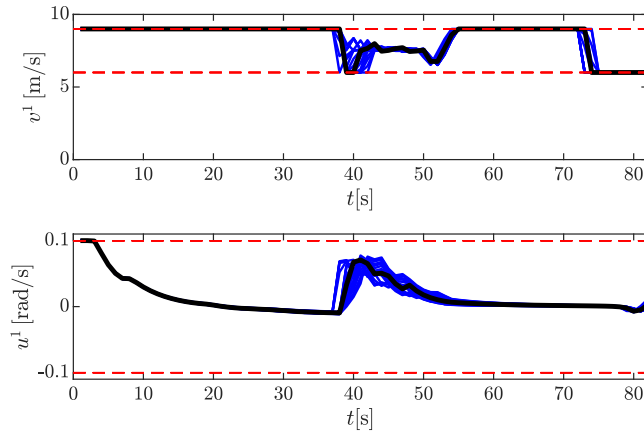


Fig. 10. The control inputs of the ownship (i.e., the linear velocity and angular velocity) and their boundaries for the scenario-tree MPC. The nominal velocities are shown in black.

Note that for the sake of clarity, in this paper, we have assumed that the ownship has priority, i.e., we apply the controller only to the ownship, while the intruder is assumed to take its optimal path, potentially with some uncertainties. There are works, e.g., in [19], where the authors consider CAS for both aircraft. In the MPC scheme, this can be achieved using distributed MPC, and it can be considered as a topic for future investigation.

VI. CONCLUSION

This paper introduced a novel intent-aware collision avoidance system tailored for multi-agent aircraft engaged in horizontal maneuvering scenarios. By leveraging intent information in the form of waypoints or destinations, we proposed the use of scenario-tree model predictive control (MPC) to offer a computationally efficient and robust approach. Through simulations, these methodologies were compared to demonstrate their effectiveness in improving collision avoidance. In aircraft CAS, while dynamic programming (DP) is a common offline approach in this context, MPC can be performed entirely online during operation. This research highlights the significance of intent awareness in multi-agent systems and provides robust strategies for improving air traffic management, ensuring safe and efficient navigation in increasingly congested airspace. Future research will focus on employing DP and reinforcement learning to derive optimal policies and compare them with the method proposed in this paper.

REFERENCES

- [1] K.-Y. Chen, P. A. Lindsay, P. J. Robinson, and H. A. Abbass, "A hierarchical conflict resolution method for multi-agent path planning," in *2009 IEEE Congress on Evolutionary Computation*. IEEE, 2009, pp. 1169–1176.
- [2] L. Jaeger, C. Gogu, S. Segonds, and C. Bes, "Aircraft multidisciplinary design optimization under both model and design variables uncertainty," *Journal of Aircraft*, vol. 50, no. 2, pp. 528–538, 2013.
- [3] K. Gopalakrishnan and H. Balakrishnan, "Control and optimization of air traffic networks," *Annual Review of Control, Robotics, and Autonomous Systems*, vol. 4, pp. 397–424, 2021.
- [4] K. D. Julian, J. Lopez, J. S. Brush, M. P. Owen, and M. J. Kochenderfer, "Policy compression for aircraft collision avoidance systems," in *2016 IEEE/AIAA 35th Digital Avionics Systems Conference (DASC)*. IEEE, 2016, pp. 1–10.
- [5] X. Zhang, Y. Liu, Y. Zhang, X. Guan, D. Delahaye, L. Tang *et al.*, "Safety assessment and risk estimation for unmanned aerial vehicles operating in national airspace system," *Journal of Advanced Transportation*, vol. 2018, 2018.
- [6] J. N. Yasin, S. A. Mohamed, M.-H. Haghbayan, J. Heikkonen, H. Tenhunen, and J. Plosila, "Unmanned aerial vehicles (UAVs): Collision avoidance systems and approaches," *IEEE Access*, vol. 8, pp. 105 139–105 155, 2020.
- [7] J. Borenstein, Y. Koren *et al.*, "The vector field histogram-fast obstacle avoidance for mobile robots," *IEEE transactions on robotics and automation*, vol. 7, no. 3, pp. 278–288, 1991.
- [8] Q. Quan, R. Fu, and K.-Y. Cai, "Practical control for multicopters to avoid non-cooperative moving obstacles," *IEEE Transactions on Intelligent Transportation Systems*, vol. 23, no. 8, pp. 10 839–10 857, 2021.
- [9] Y. Gao and D. Li, "Unmanned aerial vehicle swarm distributed cooperation method based on situation awareness consensus and its information processing mechanism," *Knowledge-Based Systems*, vol. 188, p. 105034, 2020.
- [10] L. Palmer and J. Engelbrecht, "Co-operative collision avoidance for unmanned aerial vehicles using both centralised and decoupled approaches," *IFAC-PapersOnLine*, vol. 53, no. 2, pp. 10 208–10 215, 2020.
- [11] X. Wang, M. C. Gurfsoy, T. Erpek, and Y. E. Sagduyu, "Learning-based UAV path planning for data collection with integrated collision avoidance," *IEEE Internet of Things Journal*, vol. 9, no. 17, pp. 16 663–16 676, 2022.
- [12] B. Lindqvist, S. S. Mansouri, A. A. Agha-mohammadi, and G. Nikolakopoulos, "Nonlinear MPC for collision avoidance and control of UAVs with dynamic obstacles," *IEEE Robotics and Automation Letters*, vol. 5, no. 4, pp. 6001–6008, 2020.
- [13] R. Kelley, A. Tavakkoli, C. King, M. Nicolescu, and M. Nicolescu, "Understanding activities and intentions for human-robot interaction," in *Human-Robot Interaction*. IntechOpen, 2010, pp. 288–305.

- [14] M. Bowman, S. Li, and X. Zhang, "Intent-uncertainty-aware grasp planning for robust robot assistance in telemanipulation," in *2019 International Conference on Robotics and Automation (ICRA)*. IEEE, 2019, pp. 409–415.
- [15] I. Ranatunga, S. Cremer, D. O. Popa, and F. L. Lewis, "Intent aware adaptive admittance control for physical human-robot interaction," in *2015 IEEE International Conference on Robotics and Automation (ICRA)*. IEEE, 2015, pp. 5635–5640.
- [16] C. Huang, L. Yao, X. Wang, Q. Z. Sheng, S. Dustdar, Z. Wang, and X. Xu, "Intent-aware interactive internet of things for enhanced collaborative ambient intelligence," *IEEE Internet Computing*, vol. 26, no. 5, pp. 68–75, 2022.
- [17] M. J. Kochenderfer, J. E. Holland, and J. P. Chryssanthacopoulos, "Next generation airborne collision avoidance system," *Lincoln Laboratory Journal*, vol. 19, no. 1, pp. 17–33, 2012.
- [18] M. J. Kochenderfer and J. Chryssanthacopoulos, "Robust airborne collision avoidance through dynamic programming," *Massachusetts Institute of Technology, Lincoln Laboratory, Project Report ATC-371*, vol. 130, 2011.
- [19] S. Stroeve, "What matters in the effectiveness of airborne collision avoidance systems? Monte Carlo simulation of uncertainties for TCAS II and ACAS Xa," *Aerospace*, vol. 10, no. 11, p. 952, 2023.
- [20] D. Bertsekas, *Dynamic programming and optimal control: Volume I*. Athena scientific, 2012, vol. 4.
- [21] W. B. Powell, *Approximate dynamic programming: Solving the curses of dimensionality*. John Wiley & Sons, 2007, vol. 703.
- [22] E. Klintberg, J. Dahl, J. Fredriksson, and S. Gros, "An improved dual Newton strategy for scenario-tree MPC," in *IEEE 55th Conference on Decision and Control (CDC)*, 2016, pp. 3675–3681.
- [23] A. B. Kordabad, H. N. Esfahani, A. M. Lekkas, and S. Gros, "Reinforcement learning based on scenario-tree MPC for ASVs," in *2021 American Control Conference (ACC)*. IEEE, 2021, pp. 1985–1990.
- [24] A. B. Kordabad, M. Zanon, and S. Gros, "Equivalence of optimality criteria for Markov decision process and model predictive control," *IEEE Transactions on Automatic Control*, vol. 69, no. 2, pp. 1149–1156, 2023.
- [25] K. D. Julian and M. J. Kochenderfer, "Guaranteeing safety for neural network-based aircraft collision avoidance systems," in *2019 IEEE/AIAA 38th Digital Avionics Systems Conference (DASC)*. IEEE, 2019, pp. 1–10.
- [26] L. E. Dubins, "On curves of minimal length with a constraint on average curvature, and with prescribed initial and terminal positions and tangents," *American Journal of mathematics*, vol. 79, no. 3, pp. 497–516, 1957.
- [27] D. A. Anisi, "Optimal motion control of a ground vehicle," Ph.D. dissertation, Citeseer, 2003.
- [28] X.-N. Bui, J.-D. Boissonnat, P. Soueres, and J.-P. Laumond, "Shortest path synthesis for dubins non-holonomic robot," in *Proceedings of the 1994 IEEE International Conference on Robotics and Automation*. IEEE, 1994, pp. 2–7.